Can. J. Remote Sensing, Vol. 31, No. 6, pp. 421–431, 2005

Characterization of the diminishing accuracy in detecting forest insect damage over time

Michael A. Wulder, Robert S. Skakun, Caren C. Dymond, Werner A. Kurz, and Joanne C. White

Abstract. The goal of this project was to determine the ability to detect forest insect disturbances occurring over a 6 year period using a remote sensing change detection approach. The study area in central British Columbia, Canada, has been experiencing an epidemic outbreak of bark beetles. The actual location and number of trees attacked by mountain pine beetle (*Dendroctonus ponderosae* Hopkins) were determined by annual surveys using a helicopter and a global positioning system (GPS). In this study, mountain pine beetle red-attack trees, infested between 1995 and 2001, were detected with an enhanced wetness difference index (EWDI), which was created using a 1995 and 2001 Landsat image pair. Red-attack damage was detected with an accuracy (true positive rate) of 74% using all years of the helicopter GPS survey data as validation. Assessments of the classification were subsequently undertaken that compared the EWDI-derived red-attack locations to each year of available validation data. The results of this analysis showed that recent red-attack damage was detected with greater accuracy than older red-attack damage (with an accuracy decline of approximately 15% over the 6 year period). The greatest accuracy was obtained for the most recent 2 years of attack, namely 2000 and 2001, with a red-attack detection accuracy of 81%.

Résumé. L'objectif de ce projet visait à déterminer le potentiel d'une approche basée sur la télédétection des changements pour la détection des perturbations causées à la forêt par les insectes durant une période de 6 ans. La zone d'étude, située au centre de la Colombie-Britannique, Canada, a connu une infestation de dendroctones du pin. La localisation et le nombre d'arbres affectés par le dendroctone du pin ponderosa (*Dendroctonus ponderosae* Hopkins) ont été déterminés par le biais de relevés annuels effectués à l'aide d'un hélicoptère et d'un système de positionnement global (GPS). Dans cette étude, les arbres affectés sévèrement par le dendroctone du pin ponderosa, infestés entre 1995 et 2001, ont été détectés à l'aide de l'indice EWDI (« enhanced wetness difference index »), conçu à partir du couplet d'images Landsat de 1995 et 2001. Les dommages au stade rouge ont été détectés avec une précision (taux positif réel) de 74 % en utilisant toutes les années de données de relevés GPS pour la validation. Des évaluations de classification ont été réalisées subséquemment qui comparaient les sites au stade rouge dérivés par EWDI par rapport à chaque année de données de validation disponibles. Les résultats de cette analyse ont montré que les dommages récents au stade rouge ont été détectés avec une plus grande précision que les dommages plus anciens au stade rouge (avec une diminution de précision approximative de 15 % au cours de la période de 6 ans). La plus grande précision a été obtenue dans le cas de la plus récente attaque de deux ans : 2000 et 2001, avec une précision de détection au stade rouge de 81 %.
[Traduit par la Rédaction]

Introduction

The design of efficient forest change monitoring programs can benefit from an understanding of the ability of remote sensing image analysis to detect disturbance events. Remotely sensed instruments collect data at a wide range of scales over a broad range of spectral sensitivities, thereby facilitating a plethora of monitoring options for many types of disturbance and change (Treitz and Rogan, 2004). The ability to measure and monitor the dynamics of forest ecosystems is of critical importance for forest managers, analysts, and modellers (e.g., Conkling et al., 2002; Smith, 2002; MacFarlane and Patterson Meyer, 2005). A large forested country such as Canada requires efficient and accurate change detection methods to meet the increasing requirements for reporting and the political need to fulfill obligations of international treaties such as the Convention on Climate Change (Kyoto Protocol) and the Convention on Biological Diversity. For example, Canada's National Forest Carbon Monitoring, Accounting and Reporting System (Kurz and Apps, in press) uses annualized information on impacts of forest insects and other disturbances gathered from a wide range of data sources.

Traditional forest management practices in Canada have relied on manual methods (e.g., ground surveys, airphoto interpretation) to update forest inventories. Although these techniques are effective, they are expensive and therefore inventories are updated relatively infrequently (Gillis and Leckie, 1993). Since forest disturbances can quickly change the quantity and condition of forest resources and often occur over time intervals shorter than the update cycles of traditional forest inventories, forest monitoring programs do not typically rely on

---

Received 24 December 2003. Accepted 23 August 2005.

M.A. Wulder,[1] C.C. Dymond, W.A. Kurz, and J.C. White. Pacific Forestry Centre, Canadian Forest Service, Natural Resources Canada, 506 West Burnside Road, Victoria, BC V8Z 1M5, Canada.

R.S. Skakun. Northern Forestry Centre, Canadian Forest Service, Natural Resources Canada, Edmonton, AB T6H 3S5, Canada.

[1] Corresponding author (e-mail: mwulder@nrcan.gc.ca).

forest inventories. Rather, monitoring programs use alternative data sources (e.g., annual aerial overview surveys for forest health) to provide information on forest disturbance and change (e.g., Conkling et al., 2002).

Forest damage caused by insects is one example of a disturbance that requires a rapid approach to forest health monitoring (e.g., Safranyik, 2004). Information on insect infestations must be provided quickly in order for control and mitigation activities to be implemented effectively. The successful monitoring of insect damage is further confounded by the fact that the temporal and spatial dynamics of forest insect impacts vary between years and become less visible over time. The current epidemic of mountain pine beetle (*Dendroctonus ponderosae* Hopkins) in British Columbia, Canada, is an example of the need for timely detection and mapping of insect damage. Although the current outbreak of beetles is impossible to control at this stage, having affected 7 089 902 ha in 2004 (Westfall, 2005), aggressive control tactics are still being implemented in some areas of the province (along the leading edge of the infestation; British Columbia Ministry of Forests, 2005). In these areas, rapid detection and mapping of beetle damage are necessary to remove infested trees prior to the flight of beetle offspring (McMullen et al., 1986). On a larger scale, detailed mapping of the damage caused by the beetle is required for salvage operations and for research into the longevity of the killed trees for commercial purposes (Wulder et al., 2004).

Satellite imagery provides synoptic data for the detection and assessment of insect disturbance (Rencz and Nemeth, 1985; Franklin, 1989; Franklin and Raske, 1994; Chalifoux et al., 1998). Insect disturbances in forested areas are often identified as changes in the spectral response pattern of trees that are either defoliated or killed. The negative effects of insect activities can be discerned once populations become epidemic. Immediately following a successful attack by mountain pine beetles, the host tree dies and about 12 months later the tree crown becomes red (red-attack stage) (Safranyik et al., 1974) (**Figure 1**). The red needles then drop, at varying rates, over the subsequent 2 or 3 year period (grey-attack stage) (Murtha, 1978; Wulder et al., 2004).

Historically, millions of trees and hundreds of thousands of hectares have been affected in British Columbia (Wood and Unger, 1996). At the provincial scale, two recent epidemics of mountain pine beetle have been recorded: the first one peaked from 1982 to 1985 (Wood and Unger, 1996), and the second started in 1999 and continued to increase as of 2004 (Westfall, 2005; Taylor and Carroll, 2004). On individual landscapes, mountain pine beetle infestations can persist for more than 10 years as the beetles spread from stand to stand and tree to tree (Wood and Unger, 1996). During that time, the beetle infestations can directly or indirectly (through mitigation efforts) cause mortality in hundreds or thousands of trees each year. Beetle populations may decline when there are fewer suitable hosts or when unseasonably cold temperatures result in beetle mortality. Mountain pine beetle population dynamics are a complex interaction among the insect, available hosts, climate, and other factors (Safranyik et al., 1974). Collins and Woodcock (1996) suggest that a useful approach to mapping distinct forest canopy changes, or tree mortality, is to transform Landsat data into three-dimensional space as brightness–greenness–wetness. In a recent study, Skakun et al. (2003) used this transformation to generate an enhanced wetness difference index (EWDI) using two dates of Landsat imagery collected in subsequent years (2000 and 2001). This study demonstrated that different values of the EWDI corresponded to red-attack damage caused by mountain pine beetle; a threshold of the EWDI pixels yielded a classification accuracy for red-attack damage that varied with increasing numbers of red-attack trees, namely 73% for groups of 10–29 red-attack trees and 78% for groups of 30–50 red-attack trees. Although the results of that

Figure 1. Two isolated patches of red-attack trees resulting from infestation of mountain pine beetle.

study indicated that EWDI could be a useful procedure for estimating red-attack on an annual basis, operational resources or logistical considerations may preclude the collection of imagery every year. Therefore, it is necessary to investigate the reliability of the EWDI approach for detecting red-attack over several years of beetle infestation (e.g., with a gap of 2 or more years between image dates), thereby allowing a longer time period between image acquisition dates.

The purpose of this study was to quantify the reduction in the detectability of insect infestation over time using an established technique for detecting mountain pine beetle red-attack damage from a time series of remotely sensed data. The EWDI change detection approach was applied to an area of repeated mountain pine beetle infestation located in central British Columbia, Canada. Aerial surveyors have been recording the global positioning system (GPS) locations of red-attack trees over the study area annually since 1995. In this study, we evaluated the accuracy with which survey points of red-attack damage, collected annually between 1995 and 2001, could be detected based on the analysis of a 1995 and 2001 Landsat image pair.

Methods

Study area

The study area comprised a subsection of the Morice Forest District near Prince Rupert, British Columbia, Canada. The area covered approximately 5900 km^2 (82 km east–west by 72 km north–south), centred at latitude 54°09′04.4′′N and longitude 126°33′32.1′′W (**Figure 2**). The topography is variable, with rolling hills to the north and east, becoming more mountainous in the southwest. The climate is continental but moderated by a coastal marine influence. Stands dominated by lodgepole pine (*Pinus contorta* var. *latifolia*) accounted for approximately 65% of the forested land base; the average age of these stands was 116 years in 2000. Other tree species include white spruce (*Picea glauca* (Moench) Voss), subalpine fir (*Abies lasiocarpa* (Hook.) Nutt.), western red cedar (*Thuja plicata* Donn.), balsam fir *(Abies balsamea* (L.) Mill.), western hemlock (*Tsuga heterophylla* (Raf.) Sarg.), whitebark pine (*Pinus albicaulis* Engelm.), western larch (*Larix occidentalis* Nutt.), trembling aspen (*Populus tremuloides* Michx.), and balsam poplar (*Populus balsamifera* L.).

Recent disturbances in the study area are caused by forest insects and harvesting activities (**Figure 2**). The majority of the forest damage in the study area has been attributed to mountain pine beetle, while less extensive mortality has resulted from infestations of spruce bark beetle (*Dendroctonus rufipennis)* and western balsam bark beetle (*Dryocoetes confuses*). Much of the harvesting activity in the region is clearcut and clearcut with retention. Falling and burning is a method that is also used to remove small patches of infested trees. Some cut blocks that appear in the imagery are the result of salvage of insect damage trees; this is an indirect impact of a mountain pine beetle infestation.

Data collection and image processing

Forest inventory data were stored in digital format in a geographic information system (GIS) database. The inventory data provided the principal source of information on the distribution and areal extent of forest stands circa 2001, past natural and human disturbances, and road networks in the study area. The forest inventory includes estimates of species composition (up to six different species, to the nearest 10%), stand age in years, crown closure (to the nearest 5%), stand height in metres, diameter at breast height in centimetres, and stand area in hectares (British Columbia Ministry of Sustainable Resource Management, 2002). The red-attack mapping in this study was focused only on those areas within the study area that were categorized as forest land in the GIS database.

The locations of mountain pine beetle red-attack damage were collected by helicopter surveys from 1995 to 2001. These survey flights were normally conducted from early July through August of each year, to coincide with peak periods of damage visibility (McMullen et al., 1986). Only trees with red crowns visible from the air were recorded as recent beetle damage (older defoliated trees and current green-attack trees were not included in the survey). Trained observers collected the data from a helicopter, flying at approximately 500–1000 m above ground. The surveyors observed the forest conditions, recorded the GPS location at the centre of each patch of red-attack trees, and estimated the number of damaged crowns. Each aerial survey point represented a group of up to 50 red-attack trees in an area of 0.25–0.50 ha, with cluster area, shape, and compactness not recorded (Nelson et al., 2004). For each cluster, the number of infested trees is estimated and the damaging agent is recorded. The locations and red-attack tree counts were then tabulated and stored as point data in a GIS database. This method is more accurate in terms of positioning and severity rating than traditional aerial surveys involving sketch mapping, which have been shown to overestimate the size of mountain pine beetle infestations (Harris and Dawson, 1979). Over the 1995–2001 infestation period, 9131 aerial survey points were recorded for the operational forest in the study area. Over 90% of these points represented infestation sites with less than 10 red-attack trees (**Table 1**).

The positional accuracy of the aerial-surveyed GPS points was dependent upon the quality of the GPS unit used, the helicopter height above the ground, and in some cases the speed of the helicopter. The flying height of the helicopter, coupled with the sighting angle, resulted in a potential deviation between the GPS recorded location and the actual infestation centre (**Figure 3**). Several factors contribute to point-placement errors of the aerial survey points, including off-nadir viewing and flying conditions, which can result in errors of up to 100 m. For instance, at a flying elevation of 500 m above the ground with a viewing angle of 5°, a location error of 45 m was possible. This error would be greater than the size of the Landsat pixels; therefore, validation pixels could have been

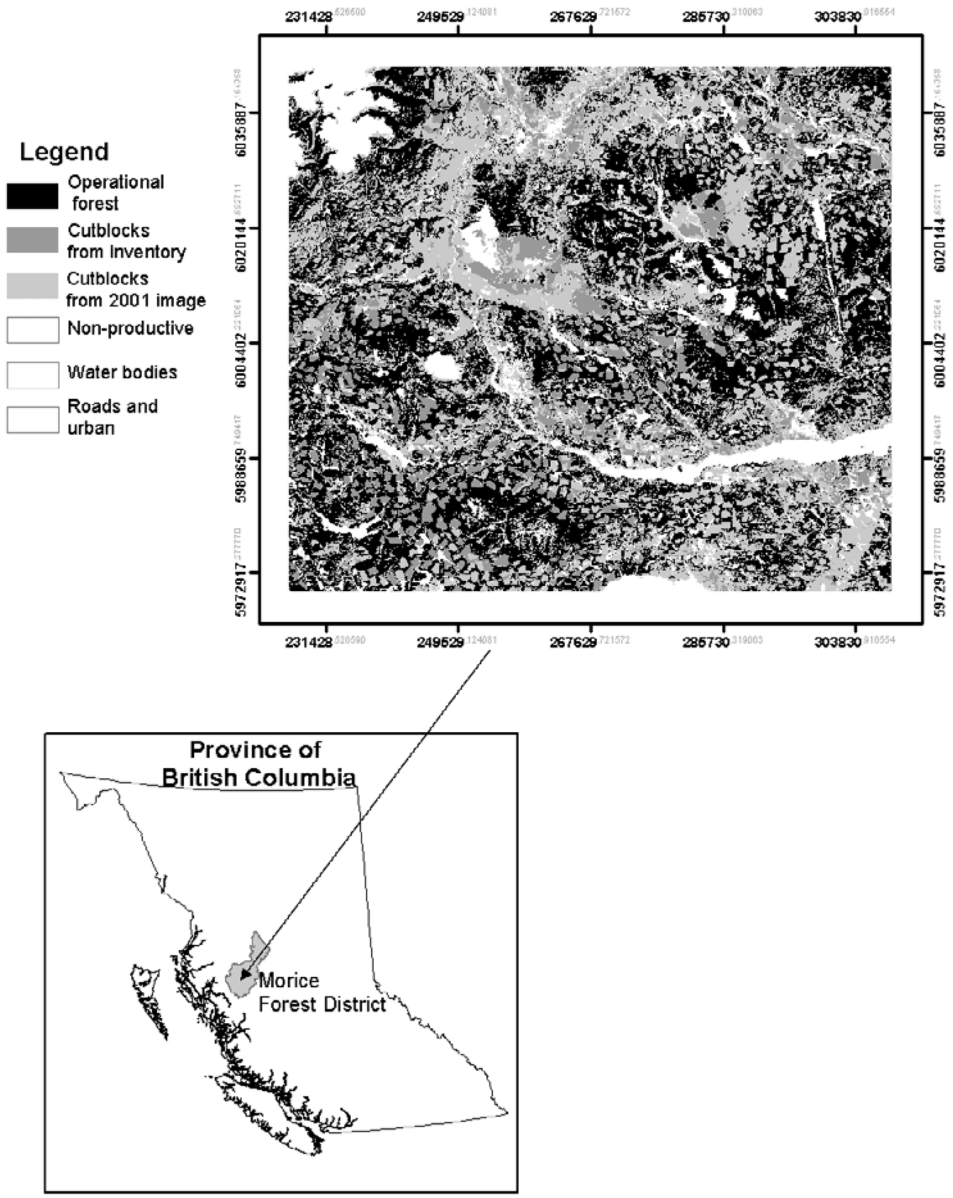

Figure 2. Study area in central British Columbia, Canada, in the Morice Forest District, centred at latitude 54°09′04.4′′N and longitude 126°33′32.1′′W. Universal Transverse Mercator (UTM) grid in metres.

mistakenly assigned as red-attack based on the aerial survey data.

To improve the quality of the calibration and validation data, we stratified the aerial survey points to reduce spectral variability caused by factors not representative of mountain pine beetle infestation. This strategy was adopted from Franklin et al. (2003), where the GIS forest inventory data were used to remove aerial survey points located in harvested areas, rocky outcrops, and fire-damaged stands. Additional aerial survey points were removed because they were located in harvest blocks discernable in the 2001 enhanced thematic mapper plus (ETM+) image. To reduce spectral influence caused by forest-edge effects, aerial survey points located near or on the edges of cut blocks, roads, or water features were also removed. From this stratified dataset, 1500 points were randomly sampled for training data, and an additional 1500 points were randomly sampled for validation (accuracy assessment). A sample of non-attack forest points was then generated using the procedures outlined in Franklin et al. (2003); a single point was randomly selected in each forest polygon that did not contain an aerial survey point. We then randomly selected 3000 of these points to obtain equal sample sizes of non-attack and red-attack points. The stratified red-attack and non-attack forest samples were used as the basis for calibration and validation of the EWDI threshold-based classification.

The red-attack classification was based on Landsat thematic mapper (TM) data from 7 September 1995 and ETM+ data

Table 1. Distribution of number of trees associated with each helicopter GPS survey point.

No. of trees estimated at a point	No. of points
1–10	8527
11–20	435
21–30	90
31–40	21
41–50	31
51–60	5
61–70	4
71–80	3
81–90	0
91–100	13
>100	2

acquired on 15 September 2001 over cloud-free regions of the Morice Forest District (path 51, row 22). The ETM+ image was obtained geometrically corrected (Wulder et al., 2002). Visual inspection of the agreement between the image and the forest inventory polygons ensured no additional geocorrections were required. The TM image was geometrically registered to the ETM+ image using 22 ground-control points with less than 0.2 pixel root mean square error. A top-of-atmosphere (TOA) reflectance correction based on the procedures of Markham and Barker (1986) was applied to each Landsat image. The TOA procedure corrected for variations in solar illumination, atmospheric transmission, and path radiance and assumes a uniform atmosphere within the image (Peddle et al., 2003). The image data were transformed from raw digital numbers to TOA reflectance values using image calibration values, radiometric ancillary information, solar zenith angle, and earth–sun distance.

Image processing consisted of image differencing and thresholding of the tasseled cap wetness transformation on a pixel-by-pixel basis. The reflectance image data were first transformed into the wetness component using an at-satellite tasseled cap transformation procedure (Huang et al., 2002). The applied TOA procedure recalibrates TM radiometry to ETM+ radiometry, allowing for at-satellite tasseled cap transformation of both Landsat images. The tasseled cap results from the two dates were then subtracted, and a linear enhancement applied, to produce the wetness index difference image. To visually highlight stands with red-attack damage, an enhanced wetness difference index (EWDI) display was generated by the 2001 wetness index using the green and blue colour guns of the display and the 1995 wetness index using the red colour gun of the display (Franklin et al., 2002; Skakun et al., 2003).

Classification of red-attack pixels was based on a threshold value of the EWDI. The red-attack threshold was developed through an iterative process, which was initiated using the mean and standard deviation of the attack training data. Using the thresholding procedures described in Skakun et al. (2003), the red-attack threshold range was then systematically altered to minimize the non-attack commission error and maximize the red-attack accuracy. Confidence intervals reported in the results were estimated based on sample size and accuracy percentage as per Czaplewski (2003).

The stand-level impact of the EWDI red-attack class was estimated using an analytical GIS approach called polygon decomposition (Wulder and Franklin, 2001; Wulder et al., 2005). Polygon decomposition is a procedure for assessing the red-attack damage conditions within a rasterized polygon. The maps produced by polygon decomposition were used in this study to illustrate the area (in hectares) and proportion (in percent) of red-attack in each forest inventory polygon. Area estimates were calculated by multiplying the total count of red-attack threshold pixels by 0.09 (1 pixel is approximately 0.09 ha). The pixel-based estimates of mountain pine beetle attack were then integrated into the GIS forest inventory. Polygon decomposition provided a practical means of determining the magnitude of the insect disturbance found within individual forest inventory polygons (Wulder et al., 2005).

Results

Accuracy of red-attack detection from 1995 to 2001

Due to the locations errors associated with the off-nadir viewing and flying position of the helicopter GPS surveys, many of the red-attack validation points were initially misclassified (high red-attack omission error). Disagreement between the placement of the GPS survey points and the pixels containing the red-attack trees impacted our ability to calibrate the EWDI thresholds, and subsequently to assess the accuracy of the resulting classification. Therefore, to account for point placement errors and enable a means to characterize the effectiveness of the EWDI approach, a 60 m buffer was generated around the red-attack validation points. For this study, a buffer distance of 60 m was chosen as an appropriate distance to account for errors in GPS survey point location; as presented in **Figure 3**, the 60 m buffer distance compensates for view angles <7° at 500 m flying height and <4° at 1000 m flying height.

The accuracy assessment results for all of the red-attack damage from 1995–2001, using the 60 m buffer distance on the helicopter GPS survey points, are summarized in **Table 2**. We have reported the accuracies in the form recommended by the British Columbia Ministry of Forests (2003). Overall accuracy was 85%, with a 90% confidence interval of 84%–86%. The true positive rate for red-attack detection was 74%, with a 90% confidence interval of 72%–76%. Red-attack omission error decreased to 26% (from an original 88%, prior to the use of the 60 m buffer around the helicopter GPS survey points).

Accuracy of red-attack detection by year

To determine how long red-attack damage can be detected after the infestation, we assessed the classified red-attack pixels using the buffered survey points, stratified by year (**Table 3**). The highest true positive rate for red-attack detection was 81% for the year 2000, and the lowest was 66% for 1996. Generally,

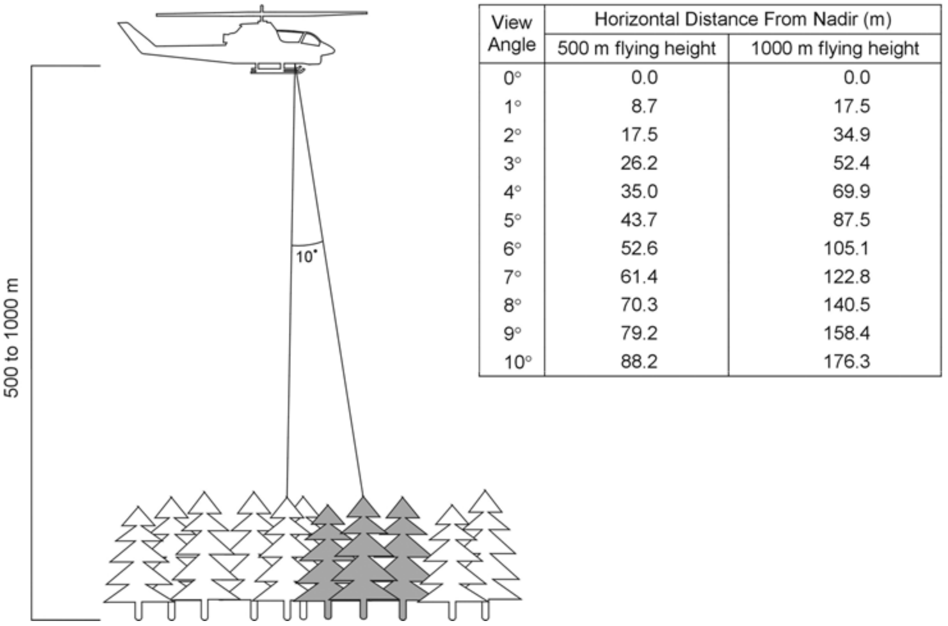

View Angle	Horizontal Distance From Nadir (m)	
	500 m flying height	1000 m flying height
0°	0.0	0.0
1°	8.7	17.5
2°	17.5	34.9
3°	26.2	52.4
4°	35.0	69.9
5°	43.7	87.5
6°	52.6	105.1
7°	61.4	122.8
8°	70.3	140.5
9°	79.2	158.4
10°	88.2	176.3

Figure 3. Illustration of how flying height and view angle can affect positional accuracy of the aerial surveyed GPS points.

Table 2. Confusion matrix of the EWDI threshold classification for red-attack and non-attack classes based on a 60 m buffer distance applied to the helicopter GPS survey validation points.

	Predicted				
	Non-attack	Red-attack	Total	Producer's accuracy (%)	Omission error (%)
Actual					
Non-attack	1448	52	1500	96.53 (true negative)	3.47 (false positive)
Red-attack	387	1113	1500	74.20 (true positive)	25.80 (false negative)
Total	1835	1165	3000		
User's accuracy (%)	78.91	95.53 (precision)			
Commission error (%)	21.09	4.46			
Overall accuracy (%)			85.36 (83.77–86.23)		

Note: This matrix pools validation points for all years (1995–2001). The 90% confidence interval is shown in parentheses for the measure of overall accuracy.

Table 3. Accuracy assessment of the EWDI red-attack threshold using the helicopter GPS validation samples stratified by year.

Time since trees turned red	Year of validation points	No. of red-attack validation points	No. of red-attack points correctly classified	True positive rate for red-attack detection (%)	Precision (%)
1–2 months	2001	204	162	79 (73–84)	76 (70–81)
1 year	2000	213	172	81 (75–86)	77 (71–82)
2 years	1999	215	165	77 (71–82)	76 (70–81)
3 years	1998	193	140	73 (66–79)	73 (66–79)
4 years	1997	290	215	74 (70–78)	81 (77–85)
5 years	1996	221	146	66 (59–72)	74 (67–80)
6 years	1995	164	112	68 (61–74)	68 (61–74)

Note: These results are based on the use of a 60 m buffer around the validation points. The 90% confidence interval is shown in parentheses.

the EWDI data detected recent red-attack damage more accurately than older red-attack damage.

An image subset illustrates the effect of time since change on the detection of red-attack (**Figure 4**). Aerial surveyors recorded a number of infestation sites from 1996 to 2001 within a lodgepole-pine-dominated polygon. The image processing and classification detected clusters of fairly light red and dark red pixels in the EWDI display. Within this polygon, the EWDI classification did not detect red-attack damage that was recorded during the 1996–1998 aerial survey flights. The

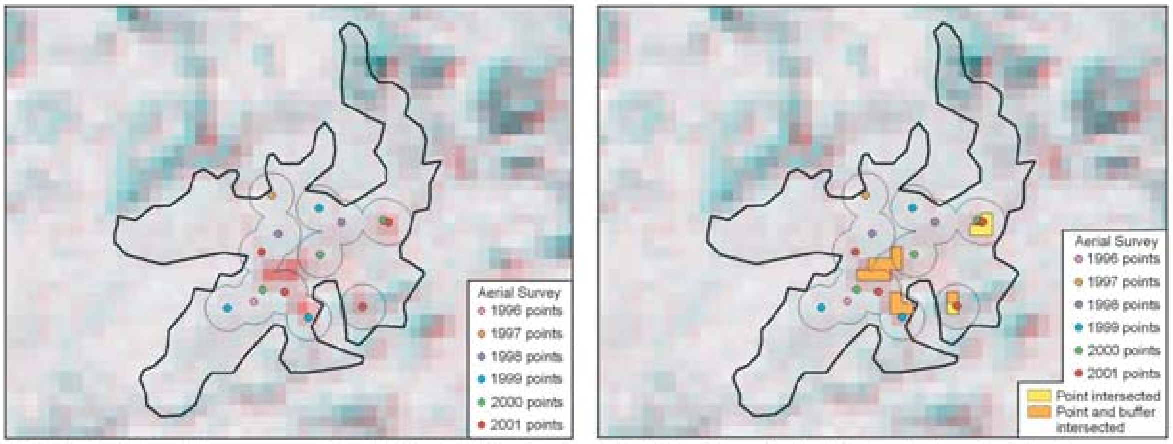

A. EWDI with aerial survey points (1996-2001) buffered 60 m

B. EWDI with red-attack threshold and aerial survey points (1996-2001)

Figure 4. Example of changing EWDI characteristics with time since attack. (A) Aerial survey points (60 m buffer around the validation points) from 1996 to 2001 overtop of EWDI display. Red-toned pixels in the forest polygon indicate red-attack damage. (B) Pixels classified as red-attack (by threshold) were displayed as yellow and orange shapes and were located close to the more recent survey flights from 1999 to 2001. See **Table 2** for details.

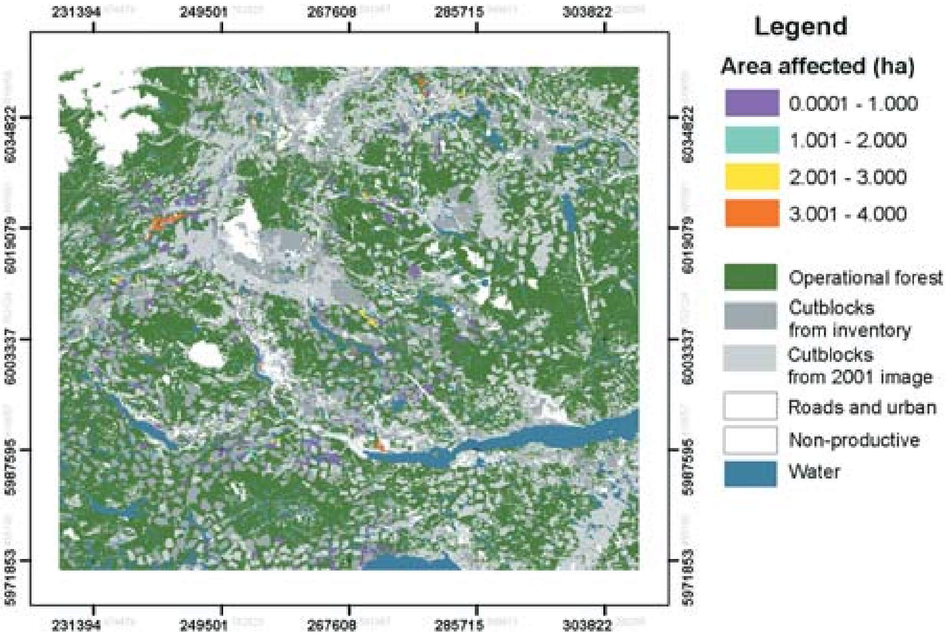

Figure 5. Landscape overview of the area attacked in each forest inventory polygon.

EWDI classification procedure did detect red-attack damage that was recorded in the 2000 and 2001 surveys. Some of the damage from the 1999 survey was also detected.

Over the entire landscape, a total of 389 ha were classified as red-attack. This represents 2.4% of the total area in forest cover polygons (16 145 ha). Most affected polygons had only a small proportion (average 3.89%) of red-attack damage; the maximum proportion of red-attack in any one polygon was 62% (with a maximum area of red-attack of 4 ha). Additional changes in the landscape resulted from harvesting, either as planned clearcut logging or sanitation and salvage logging, in response to the beetle impacts (**Figure 5**).

Discussion

An image subset illustrates the satellite imagery, classification procedure, and polygon decomposition results (**Figure 6**). In 1995, this area experienced little infestation of mountain pine beetle. By 2001, however, evidence of the presence of the beetle was noticeable, as several patches of disturbance appeared as brighter toned pixels in the colour composite. These red-attack areas appeared as light to dark red pixels in the EWDI display and had high correspondence with the 60 m circular buffers used for algorithm validation. The EWDI red-attack pixels were clustered, indicating the red-

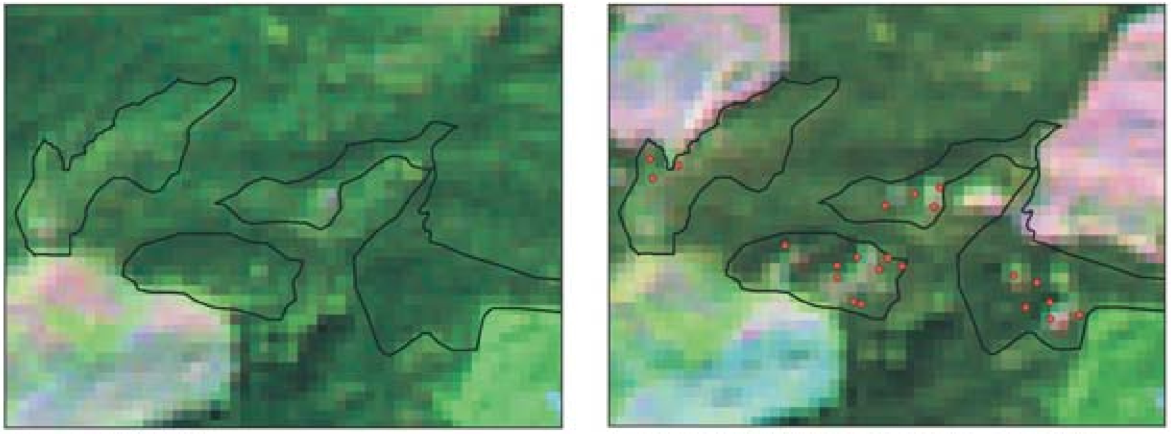

A. Landsat TM 1995

B. Landsat ETM+ 2001 with aerial survey points

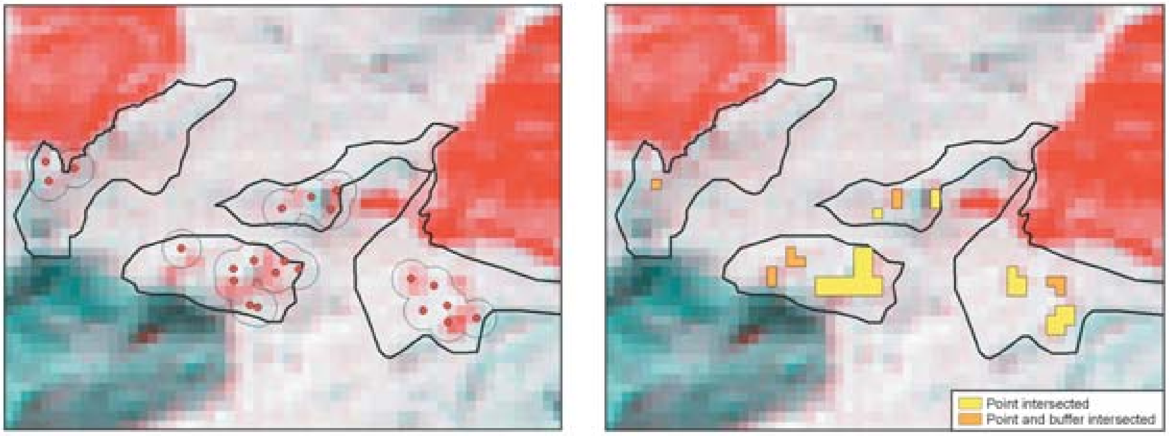

C. EWDI with aerial survey points buffered 60 m

D. EWDI with red-attack threshold

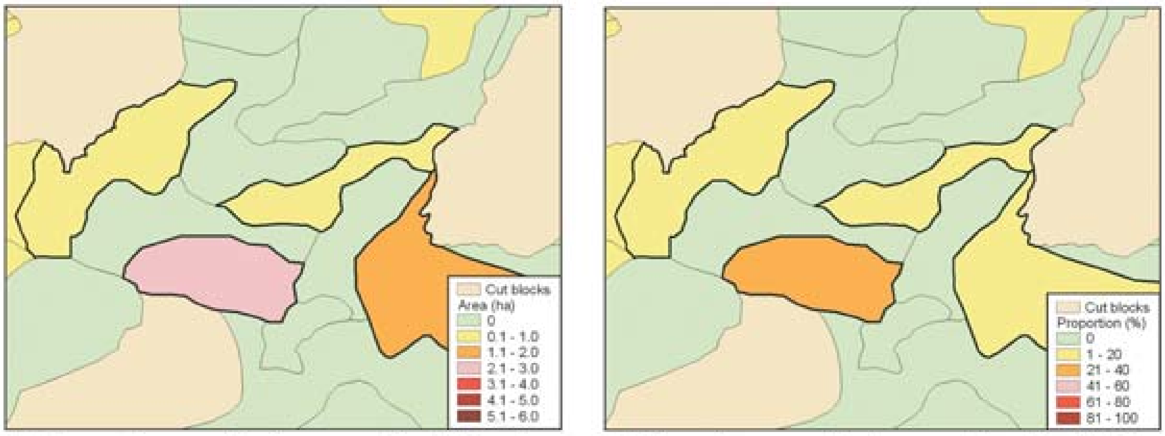

E. Polygon decomposition by area of the EWDI red-attack threshold in forest inventory polygons

F. Polygon decomposition by proportion of the EWDI red-attack threshold in forest inventory polygons

Figure 6. An example of larger patches of red-attack damage located in lodgepole-pine-dominant forest stands. Clusters of red-toned pixels in the forest polygons of the EWDI display were classified as red-attack and interpreted by the extent and intensity at the stand level.

attack trees in these forest polygons were contiguous. The magnitude of the red-attack displayed in the polygon decomposition maps showed a range of area estimates, but the proportions of red-attack relative to the forest polygon areas were fairly low.

The results indicate that red-attack damage resulting from recent infestations was detected with greater accuracy than damage resulting from older infestations. The enduring presence of red discoloured foliage, indicative of a tree that has been attacked during the past 3 years (red-attack stage), provides for a greater contrast in reflectance values (in both red and infrared wavelengths) between non-attack and attack trees. In contrast, trees attacked more than 3 years prior to the second image date will have generally faded to grey (grey-attack stage) and then subsequently lost their foliage. During the post-attack period, while the crown foliage is fading, forest successional processes are also functional, with the continued growth of understorey vegetation and the emergence of trees previously suppressed by the canopy. As the needles are shed from an attacked tree over time, the manifestation of the mountain pine beetle disturbance tends to resemble that of defoliation (Wulder et al., 2004). However, the fade rates of foliage vary, and therefore not all the trees in a forest stand will uniformly progress through each of the stages of attack (Wulder et al., 2004). This results in image pixels containing a mixture of non-attack, red-attack, and grey-attack trees, thereby making the red-attack more difficult to detect (recall **Figure 1**). Past research has indicated that the accuracy of red-attack detection increases as the number and density of red-attack trees increase (Skakun et al., 2003). This finding is also supported by research on high spatial resolution IKONOS 4 m multispectral data, where the accuracy of red-attack detection was greater where the density of red-attack damaged trees was greater (White et al., 2005).

Using the EWDI approach, large numbers of small infestation centres and larger, more contiguous areas of attack were detected. The image analysis results could be used to identify additional sites for sanitation or salvage harvesting. On a polygon basis, the proportion of area attacked was small. The ability to map damage within a predefined forest inventory polygon boundary provides a rudimentary means for assessing the local intensity of mountain pine beetle attack (Wulder et al., 2005).

The results of this study indicate that longer time intervals between images may be used to map locations of mountain pine beetle impacts, with decreasing accuracy as the time interval between images increases. As the time interval between images increases, additional change detection and disturbance attribution procedures may be required, as the trees killed by mountain pine beetle will represent a range of attack stages (including both red-attack and grey-attack stages), with the spectral characteristics increasingly resembling non-attack conditions. The condition of the individual trees and the site will also play a role in the success with which the damage caused by the mountain pine beetle can be detected over time. Site conditions, such as prolonged drought, can influence the rate at which the attacked trees will progress through the various attack stages (Safranyik, 2004), and this type of site-specific knowledge should be considered when detection and mapping are undertaken.

The practical implications of these results suggest that to detect and map mountain pine beetle damage over a longer time period, one should choose multiple image pairs over the time period in question rather than a single image pair representing the start and end years of the time period. For example, over the 1995–2001 period considered in this study, a series of EWDIs generated from multiple image pairs may have been used (e.g., 1995–1997, 1997–1999, 1999–2001). Alternatively, if resources permit, annual image pairs (e.g., 1995–1996, 1996–1997, 1997–1998, etc.) may also be used. The Landsat image archive can theoretically facilitate such retrospective analyses, although cloud-free imagery collected in the appropriate bio-window for damage detection may not always be available. This results in trade-offs in image selection, with the year and season within which the image was collected having an impact on the resultant change products. When the end-user is interested in mapping red-attack over large areas covering multiple Landsat scenes, the dates of image collection (year and month) become increasingly important.

Conclusion

This study demonstrated that Landsat images, combined with the appropriate data analysis procedures, can be used to successfully detect mountain pine beetle red-attack damage with a true positive rate of 74% (using a pair Landsat images collected 6 years apart). Annual attack information, collected via helicopter GPS surveys, facilitated the assessment of detection efficacy on an annual basis. The accuracy (true positive rate) in detecting the red-attack of a given year ranged from 66% to 81%. The more recent attack locations were captured with greater accuracy than older attack locations. This diminishing ability to detect annual impacts of an ongoing disturbance can be incorporated when designing change monitoring programs based on remotely sensed data (e.g., through selection of image dates). This approach may also provide timely information to plan forest management responses to the progression of the beetle infestation. The intended use of the attack information may also be used to guide the selection of an appropriate time interval between images intended for change detection. Higher costs may be incurred with shorter time intervals between image pairs, but higher accuracy in the ability to map mountain pine beetle attack may be expected.

Acknowledgements

Tim Ebata of the British Columbia Ministry of Forests is thanked for provision of the mountain pine beetle GPS survey data. The top-of-atmosphere calibration and correction routine used in this research was generously provided by Robert Landry of the Canada Centre for Remote Sensing. Government of Canada funding support from the Climate Change Action Fund (www.climatechange.gc.ca) and the Mountain Pine Beetle Initiative (www.mpb.cfs.nrcan.gc.ca) is gratefully noted. The Mountain Pine Beetle Initiative is a 6 year, $40 million program funded by the Government of Canada and administered by the Canadian Forest Service, Natural Resources Canada. We thank two anonymous reviewers for their constructive comments on an earlier version of the manuscript.

References

British Columbia Ministry of Forests. 2003. *Standards for research trials of mountain pine beetle attack detection using remote sensing*. Available from http://www.for.gov.bc.ca/hfp/forsite/barkbeetles/MPB%20Standards%20Feb%202503.doc [accessed 17 August 2005].

British Columbia Ministry of Forests. 2005. *British Columbia's Mountain Pine Beetle Action Plan 2005–2010*. British Columbia Ministry of Forests, Victoria, B.C. 20 pp.

British Columbia Ministry of Sustainable Resource Management. 2002. *Vegetation resources inventory: photo interpretation procedures version 2.4*. Resources Inventory Committee, British Columbia Ministry of Sustainable Resource Management, Victoria, B.C. 135 pp.

Chalifoux, S., Cavayas, F., and Grey, J. 1998. Map-guided approach for the automatic detection on Landsat TM images of forest stands damaged by Spruce Budworm. *Photogrammetric Engineering & Remote Sensing*, Vol. 64, No. 6, pp. 629–635.

Collins, J.B., and Woodcock, C.E. 1996. An assessment of several linear change detection techniques for mapping forest mortality using multitemporal Landsat TM data. *Remote Sensing of Environment*, Vol. 56, pp. 66–77.

Conkling, B.L., Hoover, C.M., Smith, W.D., and Palmer, C.J. 2002. Using forest health monitoring data to integrate above and below ground carbon information. *Environmental Pollution*, Vol. 116, pp. S221–S232.

Czaplewski, R.L. 2003. Accuracy assessment of maps of forest condition: statistical design and methodological considerations. In *Remote sensing of forest environments: concepts and case studies*. Edited by M. Wulder and S. Franklin. Kluwer Academic Publishers, Boston, Mass. pp. 115–140.

Franklin, S.E. 1989. Classification of Hemlock Looper defoliation using SPOT HRV imagery. *Canadian Journal of Remote Sensing*, Vol. 15, No. 3, pp. 178–182.

Franklin, S.E., and Raske, A. 1994. Satellite remote sensing of Spruce Budworm defoliation in western Newfoundland. *Canadian Journal of Remote Sensing*, Vol. 20, No. 1, pp. 37–48.

Franklin, S.E., Lavigne, M.B., Wulder, M.A., and Stenhouse, G.B. 2002. Change detection and landscape structure mapping using remote sensing. *Forestry Chronicle*, Vol. 78, No. 5, pp. 618–625.

Franklin, S.E., Wulder, M.A., Skakun, R.S., and Carroll, A.L. 2003. Mountain pine beetle red-attack forest damage classification using stratified Landsat TM data in British Columbia, Canada. *Photogrammetric Engineering & Remote Sensing*, Vol. 69, No. 3, pp. 283–288.

Gillis, M., and Leckie, D. 1993. *Forest inventory mapping procedures across Canada*. Forestry Canada, PNFI Information Report PI-X-114. 79 pp.

Harris, J.W.E., and Dawson, A.F. 1979. *Evaluation of aerial forest pest damage survey techniques in British Columbia*. Canadian Forestry Service, Victoria, B.C., Information Report BC-X-198. 22 pp.

Huang, C., Wylie, B., Yang, I., Homer, C., and Zylstra, G. 2002. Derivation of a tasseled cap transformation based on Landsat 7 at-satellite reflectance. *International Journal of Remote Sensing*, Vol. 23, No. 8, pp. 1741–1748.

Kurz, W.A., and Apps, M.J. In press. Developing Canada's National Forest Carbon Monitoring, Accounting and Reporting System to meet the reporting requirements of the Kyoto Protocol. *Mitigation and Adaptation Strategies for Global Change.*

MacFarlane, D.W., and Patterson Meyer, S. 2005. Characteristics and distribution of potential ash tree hosts for emerald ash borer. *Forest Ecology and Management*, Vol. 213, No. 1–3, pp. 15–24.

Markham, B., and Barker, J. 1986. Landsat MSS and TM post calibration dynamic ranges, exoatmospheric reflectances and at-satellite temperature. *EOSAT Landsat Technical Notes*, Vol. 1, pp. 3–7.

McMullen, L.H., Safranyik, L., and Linton, D.A. 1986. *Suppression of mountain pine beetle infestations in lodgepole pine forests*. Canadian Forest Service, Environment Canada, Pacific Forest Research Centre, Victoria, B.C., Information Report BC-X-276.

Murtha, P.A. 1978. Remote sensing and vegetation damage: a theory for detection and assessment. *Photogrammetric Engineering & Remote Sensing*, Vol. 44, pp. 1147–1158.

Nelson, T., Boots, B., and Wulder, M.A. 2004. Spatial–temporal analysis of mountain pine beetle infestations to characterize pattern, risk, and spread at the landscape level. In *Proceedings of the Mountain Pine Beetle Symposium: Challenges and Solutions*, 30–31 October 2003, Kelowna, B.C. Edited by T.L. Shore, J.E. Brooks, and J.E. Stone. Canadian Forest Service, Victoria, BC, Information Report BC-X-399, pp. 164–173.

Peddle, D., Teillet, P., and Wulder, M. 2003. Radiometric image processing. In *Remote sensing of forest environments: concepts and case studies*. Edited by M. Wulder and S. Franklin. Kluwer Academic Publishers, Boston, Mass. pp. 181–208.

Rencz, A.N., and Nemeth, J. 1985. Detection of mountain pine beetle infestation using Landsat MSS and simulated Thematic Mapper data. *Canadian Journal of Remote Sensing*, Vol. 11, No. 1, pp. 50–57.

Safranyik, L. 2004. Mountain pine beetle epidemiology in lodgepole pine. In *Proceedings of the Mountain Pine Beetle Symposium: Challenges and Solutions*, 30–31 October 2003, Kelowna, BC. Edited by T.L. Shore, J.E. Brooks, and J.E. Stone. Canadian Forest Service, Environment Canada, Victoria, B.C., Information Report BC-X-399, pp. 33–40.

Safranyik, L., Shrimpton, D., and Whitney, H. 1974. *Management of lodgepole pine to reduce losses from the mountain pine beetle*. Forestry Service, Environment Canada, Forestry Technical Report 1.

Skakun, R.S., Wulder, M.A., and Franklin, S.E. 2003. Sensitivity of the Thematic Mapper Enhanced Wetness Difference Index (EWDI) to detect mountain pine beetle red-attack damage. *Remote Sensing of Environment*, Vol. 86, No. 4, pp. 433–443.

Smith, W.B. 2002. Forest inventory and analysis: a national inventory and monitoring program. *Environmental Pollution,* Vol. 116, pp. S233–S242.

Taylor, S., and Carroll, A. 2004. Disturbance, forest age dynamics and mountain pine beetle outbreaks in BC: a historical perspective. In *Proceedings of the Mountain Pine Beetle Symposium: Challenges and Solutions*, 30–31 October 2003, Kelowna, B.C. Edited by T.L. Shore, J.E. Brooks, and J.E. Stone. Canadian Forest Service, Environment Canada, Victoria, B.C., Information Report BC-X-399, pp. 41–51.

Treitz, P., and Rogan, J. 2004. Remote sensing for mapping and monitoring land-cover and land-use change — an introduction. *Progress in Planning*, Vol. 61, No. 3, pp. 269–279.

Westfall, J. 2005. 2004 *Summary of forest health conditions in British Columbia*. Forest Practices Branch, British Columbia Ministry of Forests, Victoria, B.C.

White, J.C., Wulder, M.A., Brooks, D., Reich, R., and Wheate, R.D. 2005. Detection of red-attack stage mountain pine beetle infestation with high spatial resolution satellite imagery. *Remote Sensing of Environment*, Vol. 96, pp. 340–351.

Wood, C., and Unger, L. 1996. *Mountain pine beetle: a history of outbreaks in pine forests in British Columbia, 1910 to 1995*. Pacific Forestry Centre, Canadian Forest Service, Natural Resources Canada, Victoria, B.C.

Wulder, M.A., and Franklin, S.E. 2001. Polygon decomposition with remotely sensed data: rationale, methods, and applications. *Geomatica*, Vol. 55, No. 1, pp. 11–21.

Wulder, M., Loubier, E., and Richardson, D. 2002. Landsat-7 ETM+ orthoimage coverage of Canada. *Canadian Journal of Remote Sensing*. Vol. 28, No. 5, pp. 667–671.

Wulder, M.A., Dymond, C.C., and Erickson, R. 2004. *Detection and monitoring of mountain pine beetle*. Pacific Forestry Centre, Canadian Forest Service, Natural Resources Canada, Victoria, B.C., Information Report BC-X-398. 32 pp.

Wulder, M.A., Skakun, R.S., Franklin, S.E., and White, J.C. 2005. Enhancing forest inventories with mountain pine beetle infestation information. *Forestry Chronicle*, Vol. 81, pp. 149–159.